

Variability of Broad and Blueshifted Component of [OIII] λ 5007 in IZWI

J. Wang

*Department of Astronomy, Beijing Normal University, NO.19, Xijiekouwai St,
Beijing, China*

J. Y. Wei

*National Astronomical Observatories, Chinese Academy of Sciences, 20A Datun
Road, Chaoyang District, Beijing, China*

X. T. He

*Department of Astronomy, Beijing Normal University, NO.19, Xijiekouwai St,
Beijing, China*

Abstract

Although the existence of asymmetrical profile of [OIII] λ 5007 has been discovered for ages, its filiation and physics are poorly understood. Two new spectra of IZWI taken on Nov 16, 2001 and on Dec 3, 2002 were compared with the spectra taken by BG92. Following results are obtained. 1)The certain variations of broad [OIII] during about 10 years separating the observations are identified. The inferred length scale of broad [OIII] emitting region ranges from 0.3pc to 3pc. By assuming a Keplerian motion in emitting region, the material emitting broad [OIII] is likely to be located at transient emission line region, between BLR and NLR. 2)We find a positive relation between the FeII emission and flux of H β (or continuum). On the other hand, the parameter RFe decreases with ionizing continuum marginally. 3)We detect a low ionized NLR in IZWI, because of the low flux ratios [OIII]_n/H β _n(\sim 1.7).

Key words: galaxies: active, galaxies: individual: IZWI, line shape and width
PACS: 98.54Gm, 32.7Jz

Email addresses: wj@bao.ac.cn (J. Wang), wjy@bao.ac.cn (J. Y. Wei),
xthe@bnu.edu.cn (X. T. He).

1 Introduction

The asymmetry of [OIII] λ 5007 profile possessing an extended wing at blueward and a sharp red falloff was mentioned by Heckman et al.(1981) and by many subsequent researches(e.g. Busko & Steiner 1988, Grupe et al. 1999, Holt et al. 2003, Tadhunter et al. 2001). On the basis of investigations on large sample, recent studies claimed that a large fraction of AGNs are of [OIII] broad components. Véron-Cetty et al.(2001) reported that, in general, a relative narrow Gaussian profile(FWHM \sim 200 – 500 km s $^{-1}$) with a blueshifted, broad Gaussian component(FWHM \sim 500 – 1800 km s $^{-1}$) is necessary to reproduce the each [OIII] profile in a number of objects(24). In addition, a peak + blue wing structure was observed in numerous objects by Zamanov et al.(2002). The authors claimed that the [OIII] profiles have a narrow, unshifted [OIII] line with a strong blue wing. Recently, Wang et al.(2004) identified a prominent blueshifted, broad [OIII] component in Narrow-Line Seyfert 1 galaxy(NLS1) SDSS J022119.84+005628.4.

So far, although the peak+blue wing structure of [OIII] has been detected in many cases, the properties of the broad [OIII] component have been rarely investigated and poorly understood. To our knowledge, only Sergeev et al.(1997) analyzed the variations of [OIII] λ 5007 blue wing in NGC 5548. The transfer function of the blue wing is narrow-peaked near 450 days with no response up to 350 days lag. One interesting question is where is the broad component of [OIII] λ 5007 from and how large is the length scale of the line emitting region. The answers are extremely benefit to further geometrical and dynamical research of emission line region in AGN.

As usual, the study of spectral variations is a powerful technology in probing the physics of AGN. Variability can help us to set constraints on the sizes of different regions of AGNs and can give information about the processes governing the variations. The object, IZWI, is the prototype of NLS1 and was discovered by Zwicky(1971). In this paper we present two new spectra of IZWI taken in 2001 and 2002. The variations of the [OIII] broad component are examined by comparing them with the spectrum taken by Boroson & Green(1992, hereafter BG92). They examined the emission line properties of a sample of 87 low redshift ($z < 0.5$) PG quasars. The spectra with relatively high S/N ratio were obtained on a number of nights in 1990 and 1991. A resolution of 6.5-7Å was measured from the comparison spectra. The resolution at this level is adequate for identifying the evident asymmetry of the [OIII] λ 5007 line.

The paper is organized as follows. The observations and data reduction technique are described in §2. Section 3 contains the results of spectral comparison and underlying implications.

2 Observation and data reduction

The two spectra were taken on November 16, 2001 and December 3, 2002. The observations were carried out with the NAOC 2.16m telescope at the observatory of Xinglong and the OMR spectrograph, using a Tektronix 1024×1024 CCD as detector. Two different 6001 mm^{-1} gratings, blazed at 5500\AA and 5000\AA , were used in observation taken in 2001 and in 2002 respectively. Both grating give a dispersion of about $100\text{\AA} \text{ mm}^{-1}$. The slit was oriented in the north-south direction for both observations and we attempted to observe as close to the meridian as possible. Both observations were made through a $2''$ slit which produced a resolution of $\sim 6\text{\AA}$ as measured from the night sky lines. This set-up caused that the spectral resolution is identical with that of BG92 at greatest degree. In the observation taken in 2001, two exposures were performed. The exposure time of each frame was 2000s. The two frames were combined prior to extraction in order to enhance the S/N ratio and eliminate the contamination of cosmic-ray easily. Only one frame with exposure time 3000s was obtained in the observation taken in 2002.

The unprocessed frames were reduced by standard CCD procedure using IRAF package. The CCD reductions include bias subtraction, flatfield correction and cosmic-ray removal. The wavelength calibration was carried out using helium-neon-argon lamps taken at the beginning and end of each exposure. The resulting wavelength accuracy is better than 1\AA . Two or three KPNO standard stars(Massey et al. 1988) were observed per night for carrying out the flux calibration. Each of extracted spectra was transformed to rest frame in terms of the redshift determined by fitting the narrow peak of the $H\beta$ line to a Gaussian.

2.1 FeII subtraction and measurements

It is clear from the inspection of the spectra that the FeII emission is a complicating factor in measuring line parameters. In order to reliably model the line profiles it is necessary to appropriately model the FeII complex. The contamination of the FeII complex is well subtracted by the FeII template which is the FeII emission in IZWI and is described by BG92. Briefly, the template is a two-dimensional function of FWHM and of intensity of the FeII blends. The detailed procedure making the FeII template can be found in BG92. The best subtraction of the FeII blends is derived by searching in the parameter space and requires a slick continuum at blue of $H\beta$ and between 5100\AA and 5500\AA . From each spectrum the best-fit FeII spectrum is subtracted. These FeII spectra and the resulting FeII-subtracted spectra are shown in Figure 1. The spectra displayed from top to bottom panel were observed by BG92,

in Nov 16, 2001(hereafter denoted as WWHI for abbreviation) and Dec 03, 2002(WWHII, for short), respectively. In each panel, the observed spectrum is displayed by the upper curve. Note that these curves are offset upward arbitrarily for visibility. The FeII flux is measured between the rest wavelength 4434Å and 4684Å. The upper and lower limits of the flux of the FeII complex are obtained by carefully iterative experiments with a series of values of the FeII flux. Outside of the limits, the FeII-subtracted continuum is absolutely unacceptable.

2.2 Profile modelling and decomposition of other lines

The FeII-subtracted spectrum are used to measure the non-FeII line properties. The first step in the modelling of the spectra is to remove the continuum from each FeII-subtracted spectrum. The continuum is modelled by fitting a power law to the regions which seemed to be uncontaminated by emission lines. In the next step, the line profiles are modelled by multiple Gaussian fitting in the present work(e.g. Xu et al. 2003). The modelling is carried out by the SPECFIT(Kriss 1994) task in IRAF package. The fitting is persisted until the minimum of χ^2 , the measurement of goodness of the fitting, is achieved. In each spectrum, the profiles are modelled as follows. The each of forbidden lines [OIII] $\lambda\lambda$ 4959,5007 is synthesized from a narrow component and a broad, blueshifted component(see Oke & Lauer 1979, Véron-Cetty et al. 2004). The atomic physical relationships, $F_{5007}/F_{4959} \doteq 3$ (Storey & Zeipen 2000) and $\lambda_{4959}/\lambda_{5007} = 0.9904$, are used for reducing the number of free parameters and for improving the reliability of fitting in the modelling of both narrow and broad components. The narrow component of [OIII] is referred as [OIII]_n, and the broad component as [OIII]_b. The H β profile is reproduced by a set of three components: a narrow peak, a classical broad component with FWHM ~ 1000 km s $^{-1}$ and a very broad base (FWHM ~ 4000 km s $^{-1}$, see Sulentic et al. 2000b; Véron-Cetty et al. 2001; Marziani et al. 2003), because of the strong blue wing of the H β profile. The width of the narrow H β is forced to be identical with the width of narrow [OIII]. The narrow H β is referred as H β _n. The contribution, including the classical broad component and very broad component, is referred as H β _b. Figure 2 illustrates the modelling of the three observed spectra. The label of the spectrum in each panel from top to bottom is the same as that in Figure 1. The observed profiles are represented by light solid lines, and the modelled profiles, by heavy solid lines. In each panel, the narrow core and broad base of each line are shown by a short dashed line and a long dashed line, respectively. The residuals between the observed and the total fitted spectrum is displayed in the lower sub-panel underneath each spectrum.

3 Results and discussion

The three observations are compared with each other to investigate the variability of the profile of broad component of [OIII]. The two recent observations span only about one year, and the observation in BG92 was performed round about ten years ago. Table 1 summarizes the line properties of the principal emission lines at all epochs. In the following analysis and discussions in this paper, a constant flux of narrow core of [OIII] is assumed. Column 1 lists the indices of the observations. The indices are same as the indices in Figure 1 and Figure 2. The flux ratios $H\beta_n/[OIII]_n$ are listed in column 2, and the ratios $H\beta_b/[OIII]_n$ in column 3. Column 4 lists the normalized flux of broad [OIII] component. The velocity shifts of Gaussian peaks of broad [OIII] with respect to that of [OIII] narrow components are listed in column 5. A negative velocity corresponds to a blueshifted broad component relative to narrow component. The column 6 lists the flux ratio of FeII emission to narrow [OIII], along with the upper and lower limits. The last column lists the calculated parameter RFe. RFe is defined as the flux ratio of the FeII complex to $H\beta$. We note that no attempt has been made to correct for the contamination of the flux of narrow component of $H\beta$, because the flux of narrow $H\beta$ is expected to be constant. This definition avoids the additional errors caused by the decomposition. In addition, the WWHI and WWHII averaged parameters denoted as the index WWH are calculated. The mean values of the interesting parameters are reported in the last row of Table 1, except RFe, the ratio $H\beta_b/[OIII]_n$ and $FeII/[OIII]_n$. Note that the FWHM are excluded from Table 1, because we focus attention on flux variability of the broad [OIII] component.

3.1 Variability of broad [OIII]

By comparing the results of BG92 and WWH, we find remarkable variations of profile of broad [OIII] during the period of ten years separating the observations. The normalized flux in broad [OIII] decreased from 1.90 ± 0.22 to 1.00 ± 0.28 . In addition to the flux variability, the outflow(blueshift) $\Delta v_r([OIII])$ increased from $-701.3 \pm 44.2 \text{ km s}^{-1}$ to $-959.7 \pm 104.6 \text{ km s}^{-1}$. The change of velocity, WWH with respect to BG92, was -285.4 km s^{-1} which is evidently larger than the errorbar estimated by the multi-component modelling.

In Figure 3 we also show the residual profiles for all epochs as an additional test of line variability. The residual profiles are derived by removing the contributions of continuum, $H\beta$ and narrow component of [OIII]. The residuals are also normalized by a constant flux of narrow [OIII]. The vertical lines from bottom to top denote the centers of the modelled broad [OIII] components.

The authenticity of the variations is verified by following two pieces of evidence. In the first instance, the normalized flux in broad [OIII] remained constant in the recent two epochs. Once again, the coincident is elucidated by the superposition of the two residual spectra in Figure 3. According to this coincident, we are confident that the detected variations can not be caused by the observational fluctuations. Secondly, the flux ratios $H\beta_n/[OIII]_n$ are constant approximately in the all epochs, which agrees with the prediction of generally accepted unified model of AGN. Therefore, we infer that the identified profile variations can not be explained by the errors caused by the profile modelling.

According to the variations of broad [OIII] during about 10 years separating the observations, we conclude that the physical length scale of broad [OIII] emitting does not exceed 10 light years, corresponding to ~ 3 pc. On the other hand, the broad [OIII] is emitted from a larger region than the BLR (> 1 yr), because it has not varied during the 1 year separating the observations. Thus, the broad [OIII] emitting region is definitely situated at outside the BLR.

The radius of the broad [OIII] emitting region can only be obtained by indirect, model dependent arguments. Assuming that the gravitational force of the central black hole dominates the kinematics of the emitting region of broad [OIII], the broader profiles, with respect to the narrow profiles, indicate that the material emitting broad [OIII] should be located in NLR inner regions. The distance from central engine to the line region emitting broad [OIII] can be expressed as

$$R(\text{lt-days}) = 6.7 \times 10^{-6} \left(\frac{V_{\text{FWHM}}}{10^3 \text{ km s}^{-1}} \right)^{-2} \left(\frac{M_{\text{BH}}}{M_{\odot}} \right). \quad (1)$$

where V_{FWHM} is the FWHM of the emission profile of line emitting gas. The inferred black hole mass of IZWI is $\log(M/M_{\odot}) = 7.26 \pm 0.11$. The value was estimated based upon single epoch optical spectroscopy (Vestergaard 2002). Adopting the averaged FWHM of the broad [OIII] component $\sim 1500 \text{ km s}^{-1}$, the estimated distance is approximately about 100 lt-days.

The inferred distance means that the broad [OIII] in IZWI is most likely to be emitted in a transient emission line region (TLR) whose distance from central source is of order 100 lt-days. In fact, it is a long time to realize that there appears to be some interconnection between the classical BLR and NLR (Osterbrock & Mathews 1986, Sulentic et al. 2000a). Following this concept, a few authors investigated the properties of the TLR. For instance, by examining the profile of high order Blamer series and [OIII], the TLR, with a scale size of order 1pc and an intermediate FWHM ($\sim 1000 \text{ km s}^{-1}$), was reported in X-ray selected AGN RE J1034+396 (Mason et al. 1996). In the same object, by reproducing the observed spectra in terms of photoionization

calculations, Puchnarewicz et al.(1995) argued that the density of TLR($\sim 10^{7.5} \text{ cm}^{-3}$) is much lower than that of BLR and higher than that of NLR.

Up to now, in addition to the viral motions in gravitational potential of galaxy bulge(e.g. Nelson & Whittle 1996), two other kinds of mechanism, radial flow from nucleus(for example, Crenshaw & Kraemer et al. 2000) and radio jet expansion(e.g. Bicknell et al. 1998, Axon et al. 1998; Nelson et al. 2000), are suggested to explain the observed NLR. Both models can also give a reasonable origin of the asymmetry of [OIII]. For the first case, the observed peak+blue wing structure can be interpreted as the emission from a radial outflowing component with a speed of a few hundreds km s^{-1} associated with a disk component described by circular rotation(e.g. Kasier et al.(2000) in NGC 4151; Veilleux et al.(2001) in NGC 2992). On the other hand, on the basis of the jet expansion assumption, Nelson et al.(2000) modelled a set of long slit 2-dimensional spectra. This model reproduces the observed [OIII] profile in IZWI, if the far aside jet is obscured by galactic gas and the redshifted gas associated with near side jet lobe is optically thick(see Fig.7 in Nelson et al.(2000)). Cecil et al.(2002) used this scenario to analyze the deep spectra of NGC 1068 taken at high spatial resolution.

3.2 Variation of FeII emission

In addition to the variations of the broad [OIII], the variability of the optical FeII emission is identified by examining Table 1(see column 6). We find a positive relation between the FeII emission and flux of $\text{H}\beta_{\text{b}}$. According to the results of a great deal of AGN monitoring studies, generally, the $\text{H}\beta$ flux closely relates to the continuum luminosity(e.g. Peterson et al. 2002, Kaspi et al. 2000, Kollatschny et al. 2000). Therefore, it is expected that the emission of FeII increases with incident ionizing continuum in IZWI. On the contrary, a marginally negative relation between RFe and $\text{H}\beta$ (or continuum) flux is found in IZWI. This means that in IZWI the variations of the optical FeII blends are weaker in comparison to $\text{H}\beta$ line.

3.3 Low ionized NLR in IZWI

The line ratios of the NLR in NLS1s are always interesting parameters. The study of the NLR in NLS1 is not straightforward, however. Deblending the optical permitted lines in NLS1 is difficult because no transition between the narrow and broad components is observed. There is always large uncertainties in determining the fraction of $\text{H}\beta$ that is emitted by the NLR. In our analysis, both BG92 and WWH spectra indicate that the ratio $[\text{OIII}]_{\text{n}}/\text{H}\beta_{\text{n}}$ is approxi-

mate 1.7. Such low value implies that the ionization stage of NLR in IZWI is much lower than the generally adopted value($[\text{OIII}]_n/\text{H}\beta_n \sim 5 - 10$).

Is that an universal phenomenon in NLS1? As a matter of fact, Véron-Cetty et al.(2004) found a very low ionized NLR in IZWI from line system N3 in which most of oxygen might be in the form of non-ionization, both because of the weakness and absence of $[\text{OIII}]\lambda 5007$, $[\text{SII}]\lambda\lambda 6716, 6731$ as well as $[\text{OII}]\lambda 7324$ and because of the strength of $[\text{CaII}]\lambda\lambda 7291, 7324$ lines. Furthermore, the low ionization stage in NLS1s was supported by the studies of Rodriguez-Ardila et al.(2000). They found that, on average in NLS1s, 50% of flux of total $\text{H}\beta$ is due to emission from NLR and that the ratio $[\text{OIII}]_n/\text{H}\beta_n$ varies from 1 to 5. The model analysis carried out by Contini et al(2003) demonstrated that such fraction of the observed $\text{H}\beta$ line flux presents in the NLR flux in NLS1 galaxy Ark 564. Additionally, Wang et al.(2004) gave a ratio $[\text{OIII}]/\text{H}\beta_n \sim 1.62$ in SDSS J022119.84+005628.4 which is a recently identified NLS1 from Sloan Digital Sky Survey. All these results imply that normal broad line Seyfert 1s and NLS1s perhaps differ in ionization level of NLR. The NLS1s perhaps tend to commonly have a lower ionized NLR. Although we do not know whether it is a truth, a vast of effort, of course, will be made until the final result is achieved.

4 Conclusions

Two new spectra of NLS1 galaxy IZWI were recently taken by us and were compared with the spectrum taken by BG92. The comparison allows us to make following conclusions:

- (1) The variations of broad $[\text{OIII}]$ are identified during the ten years separating the observations. The variations indicate that in IZWI the length scale of emitting of broad $[\text{OIII}]$ does not exceed 3pc and is larger than 0.3pc. Assuming a Keplerian motion in emission region, the material emitting broad $[\text{OIII}]$ is possibly located in TLR, between BLR and NLR.
- (2) A positive relation between the FeII emission and $\text{H}\beta$ (or continuum) flux is identified in the object IZWI. Whereas, the parameter R_{Fe} marginally decreases with ionizing continuum.
- (3) In IZWI, the inferred flux ratio of narrow component of $[\text{OIII}]$ to narrow component of $\text{H}\beta$ is ~ 1.7 rather than the generally adopted value($\sim 5 - 10$). Such low value suggests that there is a low ionized NLR in IZWI.

5 Acknowledgments

The authors thank Profs. Todd. A. Boroson and Richard. F. Green for providing the BG92's spectra and FeII template. We are also grateful to Dr. Y. F. Mao, D. W. Xu & C. N. Hao for helpful discussions and suggestions. The special thanks go to the staff at Xinglong observatory for their instrumental and observing help. This work was supported by NSFC under grant 19973014.

References

- [1] Axon, D. J., Marconi, A., Capetti, A., Macchetto, F. D., Schreier, E., & Robinson, A., 1998, *ApJ*, 496, 75
- [2] Bicknell, G., Dopita, M. A., Tsvetanov, Z. I., & Sutherland, R. S., 1998, *ApJ*, 495, 680
- [3] Boroson, T. A., & Green, R. F, 1992, *ApJS*, 80, 109
- [4] Busko, I. C., & Steiner, J. E., *MNRAS*, 232, 525
- [5] Cecil, G., Dopita, M., Groves, B., Wilson, A., Ferruit, P., Pécontal, E., & Binette, L., 2002, *ApJ*, 2002, 568, 627
- [6] Condon, J. J., Hutchings, J. B., & Gower, A. C., 1985, *AJ*, 90, 1642
- [7] Crenshaw, D. m., & Kraemer, S. B., 2000, *ApJ*, 532, L101
- [8] Heckman, T. M., Miley, G. K., van Breugel, W. J. M., & Butcher, H. R., 1981, *ApJ*, 247, 403
- [9] Holt, J., Tadhunter, C. N., & Morganti, R., 2003, *MNRAS*, 342, 227
- [10] Grupe, D., Beuermann, K., Mannheim, K., & Thomas, H. -C., 1999, *A&A*, 350, 805
- [11] Kaspi, S., Smith, P. S., Netzer, H., Maoz, D., Jannuzi, B. T., & Giveon, U., 2000, *ApJ*, 533, 631
- [12] Kaiser, M. E., Bradley, L. D., Hutchings, J. B., et al. 2000, *ApJ*, 528, 260
- [13] Kollatschny, W., Bischoff, K., & Dietrich, M., 2000, *A&A*, 361, 901
- [14] Kriss, G., 1999, *ADASS*, 3, 437
- [15] Marziani, P., Sulentic, J. W., Zamanov, R., & Calvani, M., 2003, *Mem. S.A. It.* Vol. 74, 490
- [16] Mason, K. O., Puchnarewicz, E. M., & Jones, L. R., *MNRAS*, 283, 26
- [17] Massey, P., Strobel, K., Barnes, J. V., & Anderson, E., 1988, *ApJ*, 328, 315

- [18] Nelson, C. H., Weistrop, D., Hutchings, J. B., Crenshaw, D. M., Gull, T. R., Kaiser, S. B., & Lindler, D., 2000, *ApJ*, 531, 257
- [19] Nelson, C. H., & Whittle, M., 1996, *ApJ*, 217, 415
- [20] Oke, J. B., & Lauer, T. R., 1979, *ApJ*, 230, 360
- [21] Osterbrock, D. E., & Mathews, W. G., *ARA&A*, 24, 171
- [22] Peterson, B. M., et al., 2002, *ApJ*, 581, 197
- [23] Puchnarewicz, E. M., Mason, K. O., Siemiginowska, A., & Pounds, K. A., 1995, *MNRAS*, 276, 20
- [24] Rodriguez-Ardila, A., Binette, L., Pastoriza, M. G., & Donzelli, C. J., 2000, *ApJ*, 538, 581
- [25] Sergeev, S. G., Pronik, V. I., Malkov, Y. F., & Chuvaev, K. K., 1997, *A&A*, 320, 405
- [26] Storey, P. J., & Zeippen, G. J., 2000, *MNRAS*, 312, 813
- [27] Sulentic, J. W., Marziani, P., & Dultzin-Hacyan, D., 2000a, *ARAA*, 38, 521
- [28] Sulentic, J. W., Marziani, P., Zwitter, T., Dultzin-Hacyan, D., & Calvani, M., 2000b, *ApJ*, 545, 15
- [29] Tadhunter, C., Wills, K., Morganti, R., Oosterloo, T., & Dickson, R., 2001, *MNRAS*, 327, 227
- [30] Veilleux, S., Shopbell, P. L., & Miller, S. T., 2001, *AJ*, 121, 198
- [31] Véron-Cetty, M. -P., Joly, M., & Véron, P., 2004, *A&A*, 417, 515
- [32] Véron-Cetty, M. -P., Véron, P., & Goncalves, A. C., 2001, *A&A*, 327, 730
- [33] Vestergaard, M., 2002, *ApJ*, 571, 733
- [34] Xu, D. W., Komossa, S., Wei, J. Y., Qian, Y., & Zheng, X. Z., *ApJ*, 2003, 590, 73
- [35] Wang, J., Wei, J. Y., & He, X. T., 2004, *ChJAA*, 5, 415
- [36] Zamanov, R., Marziani, P., Sulentic, J. W., Calvani, M., Dultzin-Hacyan, D., Bachev, R., 2002, *ApJ*, 576, 9
- [37] Zwicky, F., 1971, Catalogue of selected compact galaxies and of post-eruptive galaxies, CIT, Pesadena

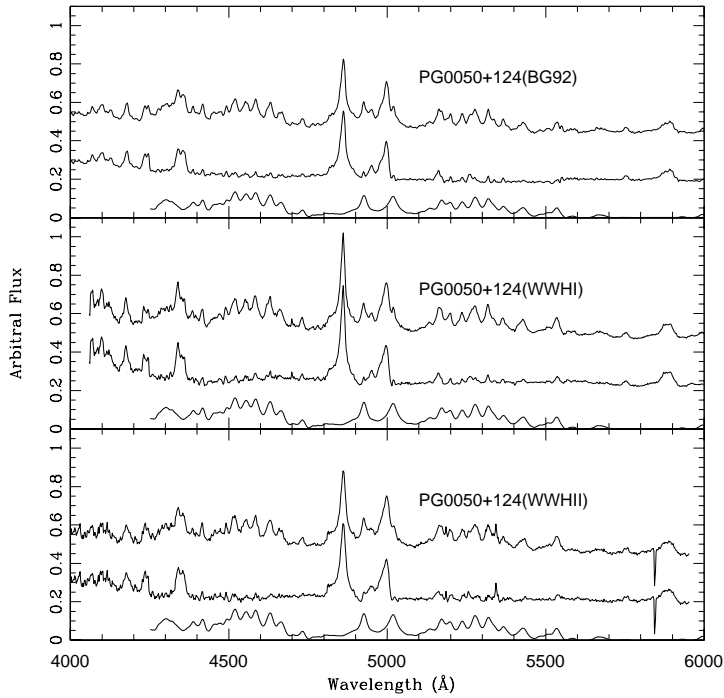


Fig. 1. An illustration of the FeII subtraction for the three independent observations. From top to bottom panel, the spectra were taken by BG92, on Nov 16, 2001 (hereafter denoted as WWHI) and on Dec 03, 2002 (WWHII), respectively. In each panel, the top curve shows the observed spectrum which is shifted upward arbitrarily for visibility. The FeII-subtracted spectrum is shown by the middle curve. The bottom curve shows the best-fitted FeII template.

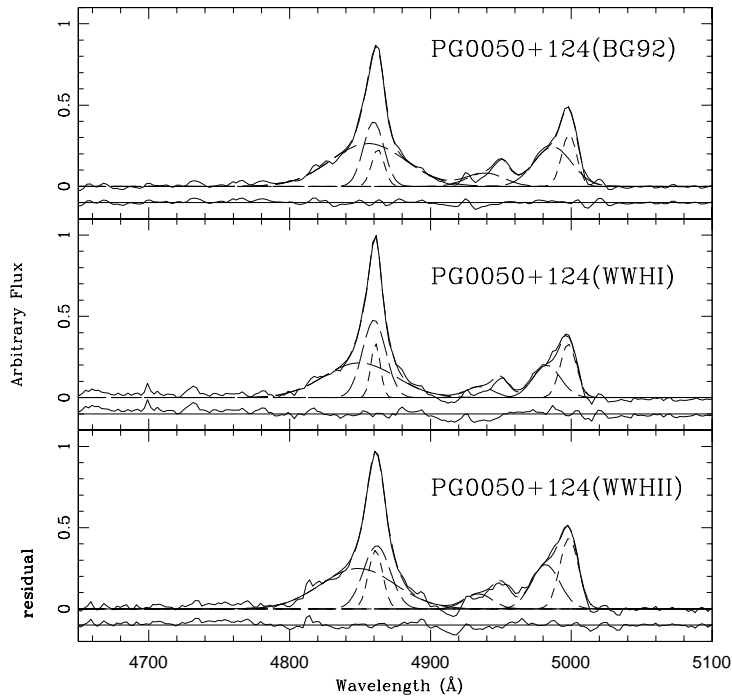


Fig. 2. Profile modelling for three observations. The label of each spectrum from top to bottom is the same as in Figure 1. The light and heavy solid line represent the observed and modelled profile, respectively. The narrow core of each line is displayed by short dashed line, the broad base by long dashed line. The residuals are shown by the lower sub-panel underneath each spectrum.

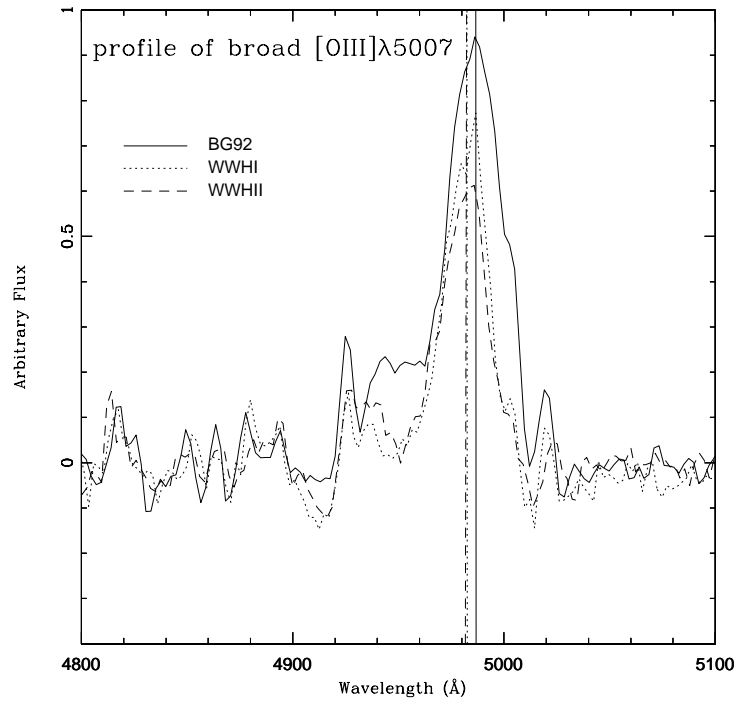


Fig. 3. Comparison of residual profiles of broad [OIII] components. The positions of center of modelled broad [OIII] are shown by lines from bottom to top.

Table 1
The Properties of Emission Lines of IZWI

Indices ^a	$H\beta_n/[OIII]_n$	$H\beta_b/[OIII]_n$	$[OIII]_b/[OIII]_n$	$\Delta v_r([OIII])^b$	$FeII/[OIII]_n$	RFe
(1)	(2)	(3)	(4)	(5)	(6)	(7)
BG92	0.60 ± 0.32	5.79 ± 0.67	1.90 ± 0.22	-701.3 ± 44.2	$12.66^{+1.27}_{-1.27}$	1.98
WWHI	0.59 ± 0.87	4.96 ± 1.04	1.04 ± 0.27	-919.1 ± 95.6	$10.96^{+0.91}_{-1.83}$	1.98
WWHII	0.64 ± 0.83	3.56 ± 0.83	0.95 ± 0.29	-1000.2 ± 112.8	$8.96^{+0.74}_{-1.49}$	2.15
WWH	0.62 ± 0.85	1.00 ± 0.28	-959.7 ± 104.6

^a The indices are identical with that in Figures 1 and 2.

^b The velocity shifts, in units of km s^{-1} , of peaks of broad components with respect to that of narrow components, where a negative velocity corresponds to a blueshifted, broad component.